JCTC Journal of Chemical Theory and Computation

ARTICLE

pubs.acs.org/JCTC

Linear Scaling Constrained Density Functional Theory in CONQUEST

Alex M. P. Sena,[†] Tsuyoshi Miyazaki,[‡] and David R. Bowler*[,†]

[†]London Centre for Nanotechnology and Department of Physics and Astronomy, University College London, Gower St, London, WC1E 6BT, United Kingdom

[‡]National Institute for Materials Science (NIMS), 1-2-1 Sengen, Tsukuba, Ibaraki 305-0047, Japan

ABSTRACT: The constrained density functional theory (cDFT) formalism is implemented in the linear scaling density functional theory (DFT) code CONQUEST. This will enable the simulation of electron-transfer processes in large biologically and technologically relevant systems. The Becke weight population scheme is chosen to define the constraint, as it enables force components to be calculated both analytically and efficiently in a linear scaling code. It is demonstrated that the imposition of a constraint is not affected by the truncation of the density matrix. Demonstration calculations are performed on charge-separated excited states in small biphenyl molecules, and cDFT is found to produce accurate energy and geometry changes for this system. The capability of the method is shown in calculations on poly phenylene-vinylene oligomers and a hydrated DNA 10-mer.

1. INTRODUCTION

Much research has been performed to elucidate how electron-transfer (ET) processes operate in biological situations, both to further understand their significance and to investigate the application of these biological roles to technological applications. Particularly well-studied examples are the processes of photosynthesis and respiration.[1,2] The transfer of electrons between porphyrin cofactors in the electron-transfer chain of respiration has inspired attempts at creating porphyrin nanowires.[3,4] While the photoinduced charge separation and recombination occurring in the photosynthetic reaction center have led to attempts to create artificial solar cells using porphyrin based systems.[5]

The difficulties in understanding the electronic structure of these large biological systems and technological analogues as well as the experimental challenges involved when investigating them have resulted in the need to study such ET processes in such systems computationally. Density functional theory (DFT)[6,7] is a widely used method for computing the ground-state properties of molecules and solids. However it is unsuited to studying electron transfer in the biological systems described above. In these systems charge transfer is usually considered as a hopping event. For the hopping of an unpaired localized electron, $D^{-}A \rightarrow DA^{-}$, the presence of the self-interaction error[8,9] can cause the electron to delocalize across multiple centers. This prevents the study of localized charge states. In addition, as DFT is a ground-state theory, the charge-separated configurations of a neutral system, $D^{-}A^{+} \rightarrow D^{+}A^{-}$, which may be excited states of the system, are not usually accessible. Finally, studying any large biological system using DFT is challenging as these systems can contain many thousands of atoms. DFT's cubic scaling results in there being a limit of approximately 1,000 atoms to the size of systems that can be studied, even with massively parallel machines.

There exists a number of ways to at least partially remedy these problems. The delocalization of unpaired electrons can be reduced through the use of hybrid functionals,[10] which reduce the self-interaction errors by introducing a portion of exact exchange. There also exists fully self-interaction corrected implementations of DFT.[11] Excited states can be studied using developments, such as linear response time-dependent DFT.[12] For the system size problem, there are approaches which, using the locality of the density matrix, allow calculations to scale linearly with the number of atoms in the system.[13] These codes can simulate systems with 10 000 atoms or more, although are often more difficult to apply in practice than conventional DFT codes. Incorporating the electron-transfer corrections described above into these linear scaling codes is challenging and may have a detrimental effect on the linear scaling. It would be desirable to have a linear scaling ET methodology to perform calculations on large biological systems.

Constrained density functional theory (cDFT)[14] is another extension to DFT, able to rectify some of the difficulties faced when studying electron transfer. In this method, an extra potential is searched for that, when added to the Kohn−Sham Hamiltonian, imposes an experimentally or physically motivated constraint on the density. It was recently shown[15] that cDFT can locate the energy minimum of the system with the addition of just one extra one-dimensional line minimization within each Kohn−Sham self-consistent step. This adds only moderate cost to a DFT calculation and does not affect the scaling with system size. A number of varied works have been performed using cDFT calculations.[16−18]

In this paper, the implementation of the cDFT formalism into the linear scaling DFT code CONQUEST[19−21] is described, and some initial calculations presented. First, the incorporation of cDFT within a linear scaling formalism is described. Then, test calculations are performed on small molecules which form the basis of future large-scale calculations to be performed. These include the hole localization in positively charged DNA base dimers and the structural changes occurring in charge separated biphenyl molecules.

Received: October 21, 2010
Published: March 07, 2011

2. METHODS

2.1. Linear Scaling DFT. Linear scaling DFT has been under development for around 15 years,[22] and there are now a number of codes available, such as SIESTA,[23] ONETEP,[24] OPENMX,[25] and CONQUEST.[26] While there are many differences in technical implementations, the basic principles in each are similar. Conventional DFT minimizes an energy expression with respect to the density $n(\mathbf{r})$ and the Kohn−Sham orbitals $\psi_i(\mathbf{r})$. Linear scaling DFT codes recast the energy functional in terms of the density matrix, $\rho(\mathbf{r},\mathbf{r}')$ and the charge density $n(\mathbf{r}) = \rho(\mathbf{r},\mathbf{r}')$. Thus direct use of the Kohn−Sham orbitals is forgone. Instead of diagonalizing the Hamiltonian directly, the energy is minimized with respect to the density matrix for a given density. The process is repeated until the input and output densities are self-consistent (or using some other update scheme, mixing density matrix and charge updates). The density matrix is formally written as

$$\rho(\mathbf{r},\mathbf{r}') = \sum_i f_i \psi_i(\mathbf{r}) \psi_i(\mathbf{r}')^* \quad (1)$$

and the energy expression is written as

$$E[n,\rho] = E_{\mathrm{KE}}[\rho(\mathbf{r},\mathbf{r}')] + E_{\mathrm{PP+Har+xc}}[n(\mathbf{r}),\rho(\mathbf{r},\mathbf{r}')] \quad (2)$$

where the density is defined as $n(\mathbf{r}) = 2\rho(\mathbf{r},\mathbf{r})$. The terms in the energy are the usual DFT ones, respectively, the kinetic, the pseudopotential(representing electron−ion interaction), the Hartree, and the exchange−correlation energies. The Kohn−Sham orbitals can be expanded in terms of localized orbitals, often known as 'support functions' ϕ_α, so that $\psi_n = \Sigma_\alpha c_n^\alpha \phi_\alpha$ giving for the elements of the density matrix:[27,28]

$$\rho(\mathbf{r},\mathbf{r}') = \sum_{\alpha\beta} \phi_\alpha(\mathbf{r}) K^{\alpha\beta} \phi_\beta(\mathbf{r}') \quad (3)$$

where $K^{\alpha\beta}$ can be formally defined as $K^{\alpha\beta} = \Sigma_n f_n c_n^\alpha c_n^\beta$. The nearsightedness of electronic matter[29] states that density correlations in a well gapped system falls off exponentially with distance. This is used to justify imposing a spatial cutoff on the density matrix such that $\rho(\mathbf{r},\mathbf{r}') \to 0$ as $|\mathbf{r}-\mathbf{r}'| \to \infty$. Consequently the number of nonzero elements in the density matrix and thus the computational cost can scale linearly with system size. The exact result is recovered as the density matrix cutoff and is increased.

Locality is imposed by restricting the support functions to lie within spherical regions and neglecting elements of the K matrix (either using a distance-based criterion, so that $K^{\alpha\beta} = 0$ when the centers of the support functions α and β are more than a specified distance apart or using a drop tolerance). The density matrix must be idempotent, to ensure that $K^{\alpha\beta}$ is a projector onto the occupied subspace during the minimization; this condition can be imposed in a variety of ways, but in the CONQUEST code, the LNV implementation of the McWeeny scheme[30−32] is used. Here K is written in terms of an auxiliary density matrix, L:$K = 3LSL - 2LSLSL$, where S is the overlap matrix between support functions, $S_{\alpha\beta} = \langle\phi_\alpha|\phi_\beta\rangle$. The energy is minimized with respect to the elements of the auxiliary density matrix L using a standard scheme (either conjugate gradients or Pulay RMM-DIIS).

The calculations performed in this paper use a double-ζ + polarization pseudoatomic-orbital basis set (apart from the PPV and DNA in water simulations, which were tested with single-zeta and single-zeta plus polarisation basis sets)[33] and the Perdew, Burke and Ernzerhof (PBE) exchange correlation functional.[34,35] Calculations can be performed using either exact diagonalization or $\mathcal{O}(N)$ density matrix minimization. This is important as exact calculations on small systems can be performed to check accuracy of $\mathcal{O}(N)$ simulations.

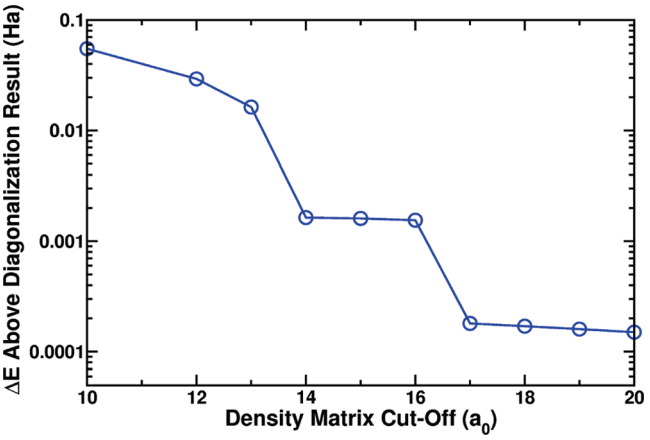

Figure 1. The convergence of energy from a $\mathcal{O}(N)$ calculation to that of a diagonalization calculation, as the density matrix cutoff is increased.

2.2. Implementation of cDFT. The recent implementation of cDFT by Wu and Van Voorhis is now outlined. Full details are found elsewhere.[15,36] It is desired to minimize the energy $E[n]$ of a system, subject to its density satisfying a constraint that the number of electrons in a given region of space around the system $w_c(\mathbf{r})$ is equal to a certain number N_c. Using the method of Lagrange multipliers, this is equivalent to minimizing a new functional W:

$$W[n,V_c] = E_{\mathrm{KS}}[n] + V_c\left(\int w_c(\mathbf{r}) n(\mathbf{r}) \mathrm{d}\mathbf{r} - N_c\right) \quad (4)$$

where the term in the bracket is the constraint and V_c the Lagrange multiplier. Minimizing W with respect to the density produces a Kohn−Sham orbital equation with an extra potential:

$$(H_{\mathrm{KS}} + V_c w_c)\phi_i = \varepsilon_i \phi_i \quad (5)$$

The minimum is located via self-consistent diagonalization of this new Hamiltonian. However at each step there is an inner loop in which the Lagrange multiplier is altered to impose the constraint on the density. In an $\mathcal{O}(N)$ scheme, only the expression for W is needed. It is recast to include the density matrix as

$$W[n,V_c] = E_{\mathrm{KS}}[n] + V_c(2\mathrm{Tr}[w_c K] - N_c) \quad (6)$$

The functional is minimized by self-consistent variation of the density matrix. However again at each step, there is an inner loop to alter the Lagrange multiplier and impose the constraint. In CONQUEST this is done using a Brent minimization algorithm to find the zero of $|\mathrm{Tr}[Kw_c] - N_c|$. The introduction of inner loops is relatively cheap, as the Hartree and exchange−correlation potentials do not need to be rebuilt each time. The inner loop also does not affect the linear scaling behavior of an $\mathcal{O}(N)$ code.

There are many different ways[15,36] of defining the constraining potential $w_c(\mathbf{r})$. The representation of this spatial function in the basis of support functions turns the constraining potential $w_c(\mathbf{r})$ into a matrix $w_{\alpha\beta}^c$, known as the weight matrix. While there is no unambiguous way of apportioning a continuous electron density to atoms, or basis functions, there are a number of schemes which sensibly formulate the spatial potential $w_c(\mathbf{r})$ using this weight

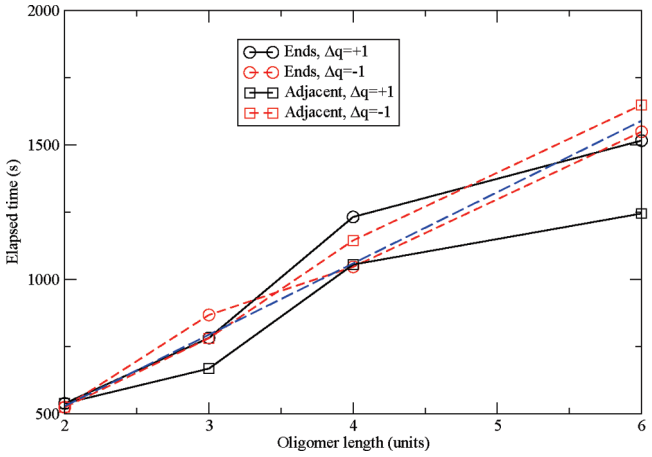

Figure 2. Total time required to find ground state for oligomers of PPV. Circles indicate charge confined to opposite ends of oligomer, and squares indicate charge confined to adjacent benzene rings. Tests were performed for differing polarities (solid and dashed lines). The long dashed line indicates linear scaling behavior extrapolated from the PPV dimer.

matrix. In our work a Becke weight scheme[37] is used:

$$w_{\alpha\beta}^{\text{Becke}} = \sum_{i\varepsilon C} \int \mathrm{d}\mathbf{r}\phi_\alpha(\mathbf{r}) w_i^c(\mathbf{r}) \phi_\beta(\mathbf{r}) \qquad (7)$$

This scheme has some advantages for use in a linear scaling code. It allows easy analytic calculation of force components, whereas schemes, such as the Löwdin populations, do not, as they require the gradient of the $S^{1/2}$ matrix. While there are schemes for finding these matrices,[38] we found them to be less practical than the Becke scheme; moreover, there can be problems decomposing S matrices with large basis sets.[38] A Cholesky decomposition does not parallelize well, and the CONQUEST code is massively parallel.

2.3. $\mathcal{O}(N)$ Calculation Convergence and Scaling. Here we present tests of the convergence of linear scaling cDFT to exact diagonalization and of the time taken to find the ground state when using linear scaling to solve.

To ensure that the truncation of the density matrix does not adversely affect the application of the constraint, a test calculation has been performed comparing the $\mathcal{O}(N)$ and diagonalization methods. cDFT is used to simulate a magnesium porphyrin molecule with the valence of the central atom constrained to be +1. Figure 1 shows how the calculated energy of the molecule for an $\mathcal{O}(N)$ cDFT calculation approaches that of a diagonalization cDFT calculation, as the range of the density matrix increases. Exact convergence occurs once the density matrix is larger than the maximum separation between two atoms in the system, approximately the diameter of the porphyrin ring here. The charge constraint was only solved to an accuracy of 10^{-4}, which will affect the total energy, as indicated in eq 6; therefore, differences between the exact diagonalization and the linear scaling solve of this order are expected, even at long density kernel ranges. We note that the accuracy is excellent for a density matrix cutoff greater than ~16 Å, which is in good agreement with recent calculations on DNA.[39]

To test the effect on the scaling of the code when performing cDFT, a series of PPV (poly phenylene-vinylene) oligomers were constructed, and excitonic states were found using cDFT. Figure 2 shows the total time to the ground state for differing exciton separations and polarities, with linear scaling behavior clearly shown. The ground-state search *without* cDFT for the dimer took 89 s and for the hexamer took 241 s, giving an overall increase in time by a factor of 6−7 for cDFT over simple DFT. This makes cDFT calculations on large systems accessible through linear scaling DFT.

Table 1. Binding Energies for DNA Base Dimers[a]

		binding energy (eV)			
dimer	separation (Å)	DFT	cDFT	DFT (B3LYP)	SIC
adenine	2.50	−1.084	−2.019	−3.533	−3.450
	6.00	0.848	0.094	0.677	−0.182
guanine	2.50	−2.321	−3.412	−3.936	−4.418
	6.00	0.691	−0.082	0.538	0.030
cytosine	2.50	−0.308	−1.558	−2.348	−6.440
	6.00	1.001	0.015	0.812	0.017
thymine	2.50	−3.421	−4.564	−5.477	−6.302
	6.00	0.955	0.102	0.625	0.013

[a] Application of a constraining potential is found to bring the energies close to the SIC values.

3. RESULTS

An $\mathcal{O}(N)$ implementation of cDFT will enable electron transfer processes to be studied in large systems. However care must be taken when selecting a system for an $\mathcal{O}(N)$ calculation. Therefore as a first step, calculations are performed on small molecules which form the basis of interesting larger systems, one example of which is given at the end.

3.1. DNA Base Pairs. The natural self-assembly of DNA into a double helix makes it a potential candidate for use as a molecular wire.[40] However, there is currently no definitive consensus on the transport properties of DNA strands.[41] Hole transfer along a DNA helix is known to be responsible for damage in the molecules, and there have been a number of studies showing high mobilities for charge carriers in DNA. However, other studies have also found DNA to be a poor charge transporter,[42−44] while a recent study has indicated the importance of self-interaction.[45] A linear scaling implementation will allow investigation of large strands of DNA base pairs, surrounded by a solvent, and will answer some these questions; initial work[39] shows promise. Here some preliminary steps are made by investigating positively charged cofacial dimers of DNA bases. Of these, guanine dimers are particularly important as they possess a low ionization potential and thus often provide a pathway through which holes can travel in DNA.[46]

When studying positively charged DNA dimers using DFT, the self-interaction error causes the hole wave function to be spread across both molecules.[47] A self-interaction corrected (SIC) DFT method has been used to localize the hole wave function on one base[47] and to investigate the change in binding energy that this produced. In this paper, the cDFT method is used to force the hole to localize on one of the bases. The binding energies for the constrained and unconstrained dimers are compared in Table 1 along with SIC values and those from a B3LYP calculation;[47] the inclusion of exchange can also mitigate self-interaction errors. The binding energies are generally negative, indicating unbound charges. We emphasize that, as cDFT is a different method to SIC, we expect only to see agreement of trends. In general, when the bases are well separated, cDFT shifts

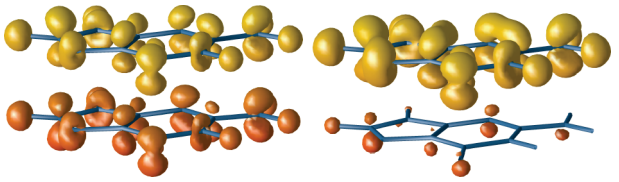

Figure 3. Charge difference density plot showing distribution of the positive hole in (left) DFT and (right) when constrained to be on the upper guanine. Color indicates height in the unit cell. The difference plotted is between the positively charged and the neutral systems.

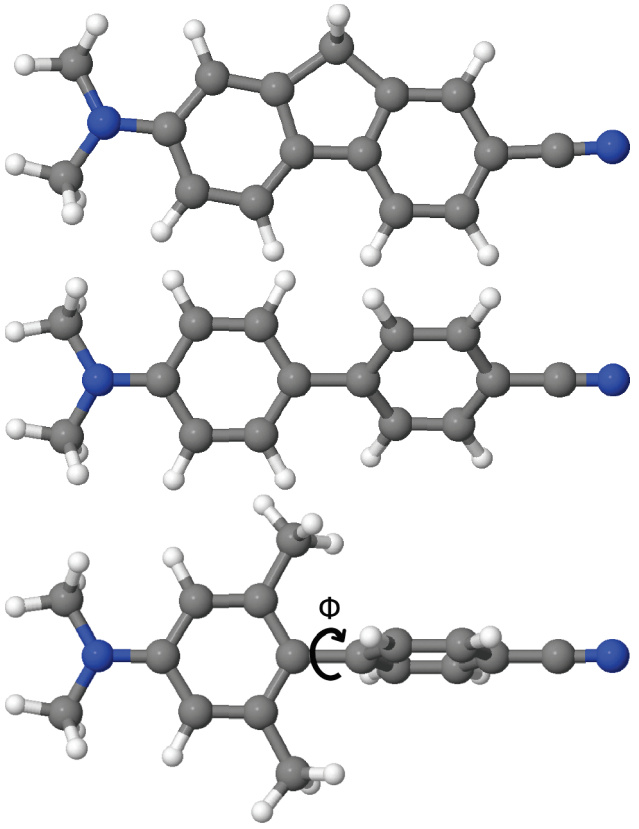

Figure 4. The structure of the three biphenyls used in the simulations here. The second (compound II) has a ground-state twist angle of 40°, and the third (compound III) has a ground-state twist angle of 70°.

Table 2. Change in Twist Angles When Charge Is Separated in Three Different Biphenyl Complexes

	twist angle (ϕ)			
molecule	AM1(Gr.St)	Expt (Ex.St)	DFT(G.St)	cDFT(Ex.St)
I	0°	0°	0°	0°
II	39°	0°	40°	0°
III	78°	40°	70°	40°

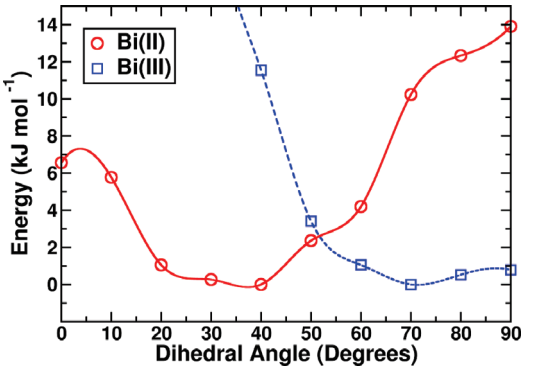

Figure 5. The twist potential (or energy profile of the twist angle) of the ground-state biphenyl II (blue line) and biphenyl III (red line) complexes.

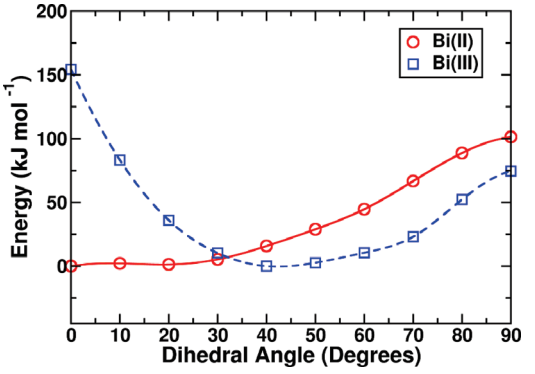

Figure 6. The excited-state twist potential for the biphenyl II and biphenyl III complexes. Complex II has an equilibrium twist angle of 0°, and III has an equilibrium angle of 40°.

the DFT binding energies toward the SIC values. However, when the bases are closer together, the cDFT results more closely resemble those from B3LYP calculations. This may be related to the problem of assigning charge to fragments which are close together,[48] though it is also quite possible that SIC methods are less accurate for close fragments.

Plotted in Figure 3 is the charge difference between a neutral and a positively charged guanine dimer for both DFT and cDFT cases. In the DFT case, the extra charge is spread across the whole dimer. When using cDFT, it is confined to just one base.

3.2. Shape Change of Biphenyls. There is considerable interest in finding molecules with switchable properties that could function as molecular electronic devices.[49−51] One of the most sought after is a molecular photoswitch whose transport properties can be changed by the application of light.[52,53] In this vein, an experimental study of three small biphenyl molecules has been made,[54] shown in Figure 4, with attention paid to the shape changes that occur when the molecule is photoexcited from its ground state to a charge-separated state. Upon photoexcitation of the molecule, the benzonitrile group (RHS of molecule) was found to act as an acceptor and become negatively charged, while the dimethylaniline group (LHS of molecule) became the positive donor. The change this caused in the equilibrium dihedral (twist) angle ϕ was then investigated. The charge-separated twist potential was found to differ from the ground-state twist potential for molecules II and III, resulting in a different equilibrium angle as shown in Table 2. Molecule I is rotationally restricted. In molecule II, the excited state has a planar geometry as opposed the 39° twist angle of the ground state. In the gas phase, the excited state of compound III has a twist angle of 40° as opposed to its ground-state angle of around 78° in nonpolar solvents.

We have used CONQUEST to perform DFT and cDFT calculations on molecules II and III. Ground-state twist potentials

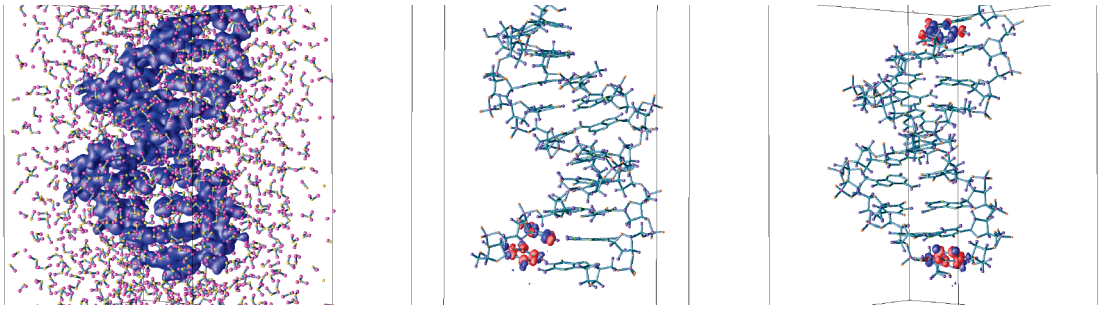

Figure 7. (a) The cell used showing water and DNA fragment with charge density of DNA fragment only shown for clarity. (b) Charge density difference (red for positive, blue for negative) for exciton confined to adjacent base pairs with DNA positions shown. (c) Charge density difference for exciton on separated base pairs with DNA positions shown.

were created by fixing the dihedral angle at various values and by allowing the other atoms of the molecule to relax. They are shown in Figure 5 and are similar to those produced using the AM1 method.[54] The twist potentials are extremely shallow, agreeing in size with previous work,[54] but the results are converged well enough to provide at least a qualitative indication of the ground-state angles, as summarized in Table 2 (column labeled DFT). cDFT was then used to create the charge separated (photoexcited) configurations. Again the twist potentials were calculated and are shown in Figure 6. This time the potentials are much deeper, and in both cases, the equilibrium angle is found to have decreased in a similar manner to the experimental observations. The new angles are seen in the column labeled cDFT in Table 2.

Having found the changes in angle, the reorganization energy for the transfer event can be calculated (though in our simulations the molecules were in the gas phase). The reorganization energy is defined as

$$\lambda = E(\mathbf{R}_{\mathrm{Gr.St}}, n_D) - E(\mathbf{R}_{\mathrm{CS.St}}, n_D) \qquad (9)$$

for the separation event. By calculating the conventional DFT energy at the constrained geometry and by using the equation above, a value of $\lambda^{\mathrm{II}}_{\mathrm{cDFT}} = 6.50$ kJ mol^{-1} and $\lambda^{\mathrm{II}}_{\mathrm{cDFTRev}} = 15.74$ kJ mol^{-1} was found for molecule II, giving an average reorganization energy of 11.12 kJ mol^{-1}. For molecule III, $\lambda^{\mathrm{III}}_{\mathrm{cDFT}} = 11.55$ kJ mol^{-1} and $\lambda^{\mathrm{III}}_{\mathrm{cDFTRev}} = 22.99$ kJ mol^{-1}, giving an average of 17.27 kJmol^{-1}. The difference in the reorganization for charge separation and recombination is likely to be due to the fact that both the initial and final states are not exactly orthogonal diabatic states of the system and the potential energy surfaces not being perfectly harmonic. Values of the reorganization energy from previous work[54] can also be extracted using the experimental charge-separated twist potentials in conjunction with the theoretical AM1 results. These yield values of $\lambda^{\mathrm{II}}_{\mathrm{Expt}} = 8.6$ kJ mol^{-1} and $\lambda^{\mathrm{III}}_{\mathrm{Expt}} = 16.0$ kJmol^{-1} in nonpolar solvents, which are most similar to the vacuum used in our simulations. The good agreement between these values and those found using cDFT is encouraging.

These results demonstrate that the energy and geometry of charge-separated excited states can be captured by creating the charge separation using cDFT. Although only a crude form of constraint altering the charge held on each half of the molecule has been used, the results are qualitatively a good fit to those from experiment. While the backward and forward reorganization energies vary significantly, their average is comparable with that from experiments on these molecules.

3.3. Charge Separation in DNA. We have previously characterized the performance of CONQUEST on a 10 base pair strand of DNA in water,[39] with a total of 3439 atoms. Here we demonstrate cDFT calculations where we create and separate an exciton on the DNA strand.

Two calculations were performed, with the charges constrained to be on adjacent bases (separated by 3−4 Å) or at opposite ends of the strand (separated within the unit cell, along the strand, by 28−29 Å, and across the unit cell separated by water by 11−12 Å). The ground state was reached *without* cDFT in 7142 s running on 64 cores connected with Infiniband (an average of 53 atoms per core, distributed automatically using our Hilbert curve algorithm).[55] For the adjacent charges, the total time was 37 487 s (an increase of about a factor of 5), while for the larger separation the total time was 54 789 s (an increase of about a factor of 8), showing that even for this large system cDFT calculations are perfectly feasible; the variations in time reflect the different paths to the minimum energy for the two potentials. We show an illustration of the DNA strand and the charge density differences for the two excitons in Figure 7. The excellent convergence shown even for this large system demonstrates that the implementation is scalable and efficient. In future work, we will explore the energetics of charge separation in a variety of biological compounds.

4. CONCLUSIONS

The cDFT formalism has been implemented into the linear scaling DFT code CONQUEST. This will enable the study of electron-transfer events in large biologically and technologically relevant systems. The Becke weight population scheme was used to form the weight matrix, due to the ease with which both the weight matrix and the analytic force components can be calculated.

Demonstration calculations were performed on four different systems. First, linear scaling of constrained DFT was demonstrated for oligomers of PPV up to 90 atoms. Then, in positively charged dimers of DNA bases, cDFT was used to correct the delocalized nature of the hole distribution and was found to shift binding energies toward those found by a fully self-interaction-corrected DFT method.

The shape changes occurring upon creation of a charge-separated excited state in two biphenyl molecules were investigated. cDFT was found to reproduce accurately the experimentally observed changes in the dihedral angle caused by photoexcitation to a charge-separated state. Following these initial results, a demonstration of cDFT in a large system (3,439 atoms) was given for the creation and separation of an exciton in a hydrated DNA 10-mer.

Future studies will include constraining the charge on an ion as it passes through the gramicidinA ion channel and investigating

its affect on the ion channel structure. They will also focus on investigating charge separation in dye molecules deposited on TiO_2 surfaces,[56,57] which have shown potential for use as artificial solar cells. It has recently been shown that linear scaling DFT calculations can address systems with millions of atoms,[58] which opens up the prospect of performing cDFT calculations on biologically relevant and important systems.

AUTHOR INFORMATION

Corresponding Author

*E-mail: david.bowler@ucl.ac.uk.

ACKNOWLEDGMENT

A.M.P.S. was supported by the IRC in Nanotechnology. D.R.B. was supported by the Royal Society. T.M. acknowledges the support from a Grant-in-Aid for Scientific Research from the MEXT and JSPS, Japan. The authors are grateful to Takao Otsuka for the positions of the DNA in water.

REFERENCES

(1) Ermler, U.; Fritzsch, G.; Buchanan, S.; Michel, H. *Structure* **1994**, *2*, 925.
(2) D'Souza, F.; Chitta, R.; Gadde, L., S.; Rogers; Karr, P.; Zandler, M.; Sandanayaka, A.; Araki, Y.; Ito, O. *Chem.—Eur. J.* **2007**, *13*, 916.
(3) Tagami, K.; Tsukada, M.; Matsumoto, T.; Kawai, T. *Phys. Rev. B: Condens. Matter Mater. Phys.* **2003**, *67*, 245324.
(4) Kocherzhenko, A.; Patwardhan, S.; Grozema, F.; Anderson, H.; Siebbeles, L. *J. Am. Chem. Soc.* **2009**, *131*, 5522.
(5) Campbell, W.; Burrell, A.; Officer, D.; Jolley, K. *Coord. Chem. Rev.* **2004**, *248*, 1363.
(6) Hohenberg, P.; Kohn, W. *Phys. Rev.* **1964**, *136*, B864.
(7) Kohn, W.; Sham, L. *Phys. Rev.* **1965**, *140*, A1133.
(8) Perdew, J. P.; Zunger, A. *Phys. Rev. B: Condens. Matter Mater. Phys.* **1981**, *23*, 5048.
(9) Zhang, Y.; Yang, W. *J. Chem. Phys.* **1998**, *109*, 2604.
(10) Becke, A. *J. Chem. Phys.* **1993**, *98*, 5648.
(11) Perdew, J. P.; Zunger, A. *Phys. Rev. B: Condens. Matter Mater. Phys.* **1981**, *23*, 5048.
(12) Marques, M.; Gross, E. *Annu. Rev. Phys. Chem.* **2004**, *55*, 427.
(13) Goedecker, S. *Rev. Mod. Phys.* **1999**, *71*, 1085.
(14) Dederichs, P. H.; Blügel, S.; Zeller, R.; Akai, H. *Phys. Rev. Lett.* **1984**, *53*, 2512.
(15) Van Voorhis, T.; Wu, Q. *Phys. Rev. A: At., Mol., Opt. Phys.* **2005**, *72*, 024502.
(16) Oberhofer, H.; Blumberger, J. *J. Chem. Phys.* **2009**, *131*, 064101.
(17) Rudra, I.; Wu, Q.; Van Voorhis, T. *J. Chem. Phys.* **2006**, *124*, 024103.
(18) Wu, Q.; Kaduk, B.; Van Voorhis, T. *J. Chem. Phys.* **2009**, *130*, 034109.
(19) Bowler, D.; Miyazaki, T.; Gillan, M. *J. Phys.: Condens. Matter* **2002**, *14*, 2781.
(20) Miyazaki, T.; Bowler, D.; Choudhury, R.; Gillan, M. *J. Chem. Phys.* **2004**, *121*, 6186.
(21) Bowler, D. R.; Choudhury, R.; Gillan, M. J.; Miyazaki, T. *Phys. Status Solidi B* **2006**, *243*, 989.
(22) Bowler, D. R.; Fattebert, J.-L.; Gillan, M. J.; Haynes, P. D.; Skylaris, C.-K. *J. Phys.: Condens. Matter* **2008**, *20*, 290301.
(23) Artacho, E.; Anglada, E.; Dieguez, O.; Gale, J.; Garcia, A.; Junquera, J.; Martin, R.; Ordejon, P.; Pruneda, J.; Sanchez-Portal, D.; Soler, J. *J. Phys.: Condens. Matter* **2008**, *20*, 064208.
(24) Skylaris, C.-K.; Haynes, P. D.; Mostofi, A. A.; Payne, M. C. *J. Chem. Phys.* **2005**, *122*, 084119.
(25) Ozaki, T.; Terakura, K. *Phys. Rev. B* **2001**, *64*, 195126.
(26) Gillan, M.; Bowler, D.; Torralba, A.; Miyazaki, T. *Comput. Phys. Commun.* **2007**, *177*, 14.
(27) Hernández, E.; Gillan, M. *Phys. Rev. B: Condens. Matter Mater. Phys.* **1995**, *51*, 10157.
(28) Hernandez, E.; Gillan, M.; Goringe, C. *Phys. Rev. B: Condens. Matter Mater. Phys.* **1995**, *53*, 7147.
(29) Prodan, E.; Kohn, W. *Proc. Natl. Acad. Sci. U.S.A.* **2003**, *102*, 11635.
(30) Li, X.-P.; Nunes, R.; Vanderbilt, D. *Phys. Rev. B: Condens. Matter Mater. Phys.* **1993**, *47*, 16.
(31) McWeeny, R. *Rev. Mod. Phys.* **1960**, *32*, 2.
(32) Bowler, D. R.; Gillan, M. *J. Comp. Phys. Commun.* **1999**, *120*, 95.
(33) Torralba, A.; Todorovic, M.; Brazdova, V.; Choudhury, R.; Miyazaki, T.; Gillan, M.; Bowler, D. *J. Phys.: Condens. Matter* **2008**, *20*, 294206.
(34) Perdew, J. P.; Burke, K.; Ernzerhof, M. *Phys. Rev. Lett.* **1996**, *77*, 3865.
(35) Torralba., A.; Bowler, D.; Miyazaki, T.; Gillan, M. *J. Chem. Theory Comput.* **2009**, *5*, 1499.
(36) Van Voorhis, T.; Wu, Q. *J. Chem. Theory Comput.* **2005**, *2*, 765.
(37) Becke, A. *J. Chem. Phys.* **1988**, *88*, 2547.
(38) Jansik, B.; Host, S.; Jorgenssen, P.; Olsen, J.; Helgaker, T. *J. Chem. Phys.* **2007**, *126*, 124104.
(39) Otsuka, T.; Miyazaki, T.; Ohno, T.; Bowler, D.; Gillan, M. *J. Phys.: Condens. Matter* **2008**, *20*, 294201.
(40) Priyadarshy, S. *Synth. React. Inorg. Met.* **2007**, *37*, 353.
(41) Endres, R.; Cox, D.; Singh, R. *Rev. Mod. Phys.* **2004**, *76*, 195.
(42) Guo, X.; Gorodetsky, A.; Hone, J.; Barton, J.; Nuckolls, C. *Nat. Nano.* **2008**, *3*, 163.
(43) Delaney, S.; Barton, J. *J. Org. Chem.* **2003**, *68*, 6475.
(44) Gomez-Navarro, C.; Moreno-Herrero, F.; de Pablo, P.; Colchero, J.; Gomez-Herrero, J.; Baro, A. *Proc. Natl. Acad. Sci. U.S.A.* **2001**, *99*, 8484.
(45) Pemmaraju, C. D.; Rungger, I.; Chen, X.; Rocha, A. R.; Sanvito, S. *Phys. Rev. B: Condens. Matter Mater. Phys.* **2010**, *82*, 125426.
(46) Kawai, K.; Kodera, H.; Osakada, T., Y; Majima *Nat. Chem.* **2009**, *1*, 156.
(47) Mantz, Y.; Gervasio, F.; Laino, T.; Parrinello, M. *J. Phys. Chem. A* **2006**, *111*, 105.
(48) Wu, Q.; Cheng, C.-L.; Van Voorhis, T. *J. Chem. Phys.* **2007**, *127*, 164119.
(49) Feldheim, D. *Nature* **2000**, *408*, 45.
(50) Qian, H.; Lua, J.-Q. *Phys. Lett. A* **2007**, *371*, 465–468.
(51) Ying Quek, S.; Kamenetska, M.; Steigerwald, M.; Joon Choi, H.; Louie, S.; Hybertsen, M.; Neaton, J.; Venkataraman, L. *Nat. Nano.* **2009**, *4*, 230–234.
(52) Sallenavea, X.; Delbaereb, S.; Vermeerschb, G.; Salehc, A.; Pozzo, J.-L. *Tetrahedron Lett.* **2005**, *46*, 3257–3259.
(53) Sauer, M. *Proc. Natl. Acad. Sci. U.S.A.* **2005**, *102*, 9433.
(54) Maus, M.; Rettig, W.; Bonafoux, D.; Lapouyade, R. *J. Phys. Chem. A* **1999**, *103*, 3388.
(55) Brazdova, V.; Bowler, D. *J. Phys.: Condens. Matter* **2008**, *20*, 275223.
(56) O'Rourke, C.; Bowler, D. R. *J. Phys. Chem. C* **2010**, *114*, 20240.
(57) Terranova, U.; Bowler, D. R. *J. Phys. Chem. C* **2010**, *114*, 6491.
(58) Bowler, D. R.; Miyazaki, T. *J. Phys.: Condens. Matter* **2010**, *22*, 074207.